



Tk 30. 329

1960 JUN 27

KFKI
10/1969

**CHARGE-STATE OSCILLATIONS
IN NEUTRON-PROTON SCATTERING**

Gy. Hrehuss, T. Czibók

**HUNGARIAN ACADEMY OF SCIENCES
CENTRAL RESEARCH INSTITUTE FOR PHYSICS**

BUDAPEST

2017

CHARGE-STATE OSCILLATIONS IN NEUTRON-PROTON SCATTERING

G. Hrehuss and T. Czibók

Central Research Institute for Physics, Budapest Hungary

Summary

Periodical state-flipping phenomena analogous to those occurring at electromagnetic excitations have been found in the case of neutron-proton scattering. The periodical charge-state flipping manifests itself as an oscillation in the energy dependence of both the total cross-section and the differential cross-section at forward proton-angles. The flipping frequency measured is in good agreement with that estimated theoretically making use of a simple model for charge-exchange processes.

Revised version of the original paper "Charge-State Flipping Phenomena in Neutron-Proton Scattering", preprint, KFKI 19/1968

CHARGE-STATE OSCILLATIONS IN NEUTRON-PROTON SCATTERING

G. H. W. H. and T. G. G.

Central Research Institute for Physics, Budapest, Hungary

Summary

Periodical charge-flipping phenomena analogous to those occurring at electro-magnetic excitations have been found in the case of neutron-proton scattering. The periodical charge-state flipping manifests itself as an oscillation in the energy dependence of both the total cross-section and the differential cross-section at forward proton angles. The flipping frequency measured is in good agreement with that estimated theoretically using as a simple model for charge-exchange processes.

Revised version of the original paper "Charge-State Flipping Phenomena in Neutron-Proton Scattering", presented, April 1958

1.3. Introduction

The periodical state-flipping is a well-known phenomenon occurring in the case of electromagnetic excitations [1] if certain conditions are fulfilled. Consider e.g. an atomic or molecular beam in which the particles have a well defined velocity and suppose that they are in one of their internal states of long enough mean-life. Assume that the transition to be investigated takes place between this state $|\beta\rangle$ and a next one $|\beta'\rangle$ which is also a long-lived state and that no other state is available either from $|\beta\rangle$ or from $|\beta'\rangle$ with the same transition frequency $\omega_{\beta\beta'}$. If the beam is shot through a cavity containing electromagnetic field with a frequency suitable to perform the transition $|\beta\rangle \leftrightarrow |\beta'\rangle$ the internal state of the particles can be changed by choosing a proper flight-time in the cavity. More precisely, the probability to find the particles emerging from the cavity in either of the two internal states involved turns out to be a periodical function of the flight-time t i.e. of the duration of interaction, and the frequency of this state flipping is $|H_{\beta\beta'}|/\hbar$ where $H_{\beta\beta'}$ is the matrix-element for the transition under cavity conditions. /For example, $H_{\beta\beta'} = \xi_0 D_{\beta\beta'}$ for electric-dipole transitions in the strong electric field ξ_0 of the cavity and $D_{\beta\beta'}$ is the dipole matrix-element for the states in question./

Similar phenomena can be expected to occur if the cavity contains but few photons /and also the atoms or molecules investigated in rare-gas form/.

The whole process can be seen, however, from a different point of view as well. The radiation field /and gas particles/ confined to the cavity can be considered as a "scatterer" which acts so as to change the initial state of the projectiles. The cross-section $\sigma_{\beta\beta'}$ of this "reaction" is energy-dependent, in the sense that it is a periodical function of the flight-time $t \sim E^{-1/2}$ where E is the kinetic energy of the projectiles.

Let's reconsider now the phenomenon as a potential possibility for nuclear processes such as neutron-proton scattering or scattering of fast nucleons on more complex nuclei. First of all, the proton and the neutron are known as different charge-states of the same entity called as nucleon.

The transition between these states which is analogous to that in the electromagnetic case would involve the emission of a charged pion. Since both the pions and the photons are Bose-particles the structure of the interaction Hamiltonians should be very similar. The emission of a pion by a free neutron cannot be realized because of the slight difference between the neutron and proton rest-masses, there is, however, a possibility for an exchange of charge-states between a proton and neutron if they approach each other for a distance less than the pion Compton wave-length. It is tempting to interpret this as an analogy to the case of a cavity having perfectly reflecting walls and containing one particle and one photon in a dynamical state /to be specified later/. The photon is unable to leave the cavity but it can change the internal state of a projectile that happened to cross this interaction region. The idea can be generalized for the case of nucleon scattering on more complex nuclei simply to the analogy of a cavity containing more than one gas-particle in dynamical equilibrium with the radiation field in it.

In what follows the idea will be developed in some more quantitative terms. The estimation of the charge state flipping frequencies for n-p and n-d scattering will be followed by a survey and analysis of experimental data to unfold the phenomenon, if exists. In order to support the existence of a periodically fluctuating cross-section contribution actually found in the energy-dependence of the total cross-section of n-p scattering above 2 MeV, more direct experiments have been performed with encouraging results. This will be described in the last but one §. of this paper. The charge-state flipping phenomena found in the case of more complex target nuclei will be described in an other article.

2 §. Calculation of the state-flipping frequencies

In the first part of this paragraph the method of the calculations will be developed. This will be followed by applications to some problems of interest as outlined in the Introduction.

2.1. Let's consider a cavity with walls perfectly reflecting the radiation closed in but transparent for the projectile that crossed it from outside. Both the projectile and the "gas-particles" in the cavity are identical so that all particles under consideration have the same set of internal states $|\beta\rangle$. The stationary states of the unified though not interacting system of particles and radiation field closed by the cavity can be specified by a state-vector $|n_1 n_2 \dots n_i \dots, \beta_0 \beta_1 \dots \beta_j \dots\rangle$ where n_i stands for the number of quanta of energy $\hbar\omega_i$ and β_j is

the quantum number characterizing the internal state the j-th particle happens to be in. Since only quantum-exchange interaction will be considered between the particles /via radiation field/ the state-vector $|\dots n_i \dots \beta_j \dots\rangle$ is factorizable. The state of the unified and interacting system is now given by the time-dependent superposition

$$\psi = \sum_{n_1} \sum_{n_2} \dots \sum_{\beta_0} \sum_{\beta_1} \dots c_{n_1 n_2 \dots \beta_0 \beta_1 \dots}(t) |n_1 n_2 \dots \beta_0 \beta_1 \dots\rangle e^{-\frac{i}{\hbar}(E_r + E_q)t} \quad /1/$$

which is due to satisfy the time-dependent Schrödinger-equation

$$(H_P + H_R + H_{int})\psi = i\hbar \frac{\partial \psi}{\partial t} \quad /2/$$

where the Hamiltonians H_P and H_R are those of the particle system and the radiation field, respectively, as

$$H_P |\beta_0 \beta_1 \dots \beta_j \dots\rangle = E_q |\beta_0 \beta_1 \dots \beta_j \dots\rangle \quad E_q = \sum_j E_{\beta_j}$$

$$H_R |n_1 n_2 \dots n_i \dots\rangle = E_r |n_1 n_2 \dots n_i \dots\rangle \quad E_r = \sum_i \hbar \omega_i \left(n_i + \frac{1}{2} \right) \quad /3/$$

H_{int} is the interaction Hamiltonian to be specified later. It is assumed that the interaction is switched on only if the projectile is within the cavity walls. Substituting Eq /1/ into Eq /2/ and taking into account Eqs/3/ one gets a coupled system of differential equations in the usual way for the amplitudes $c_{n_1 n_2 \dots \beta_0 \beta_1 \dots}(t)$ as

$$\dot{c}_{n_1 n_2 \dots \beta_0 \beta_1 \dots} = i\hbar^{-1} \sum_{n'_1} \sum_{n'_2} \dots \sum_{\beta'_0} \sum_{\beta'_1} \dots \langle n_1 n_2 \dots \beta_0 \beta_1 \dots | H_{int} | n'_1 n'_2 \dots \beta'_0 \beta'_1 \dots \rangle \cdot e^{i(\omega_{rr'} + \omega_{qq'})t} c_{n'_1 n'_2 \dots \beta'_0 \beta'_1 \dots} \quad /4/$$

where

$$\omega_{rr'} = (E_r - E_{r'}) / \hbar = \sum_i \omega_i (n_i - n'_i) \quad /5a/$$

$$\omega_{qq'} = (E_q - E_{q'}) / \hbar = \hbar^{-1} \sum_j (E_{\beta_j} - E_{\beta'_j}) \quad /5b/$$

The initial conditions to Eqs/4/ can be given by specifying the amplitudes $c_{n_1 n_2 \dots \beta_0 \beta_1 \dots}(t)$ up to the moment when the interaction is switched on i.e. for $t \leq 0$, by assumption. As for the projectile,

its initial state can be specified unambiguously while no definite values can be given to the remaining quantum numbers. The only statement one can give is that

$$\sum_{n_1} \sum_{n_2} \dots \sum_{\beta_1} \sum_{\beta_2} \dots |c_{n_1 n_2 \dots, \beta_1 \beta_2 \dots}(t < 0)|^2 = 1$$

The amplitudes $c_{n_1 n_2 \dots, \beta_1 \beta_2 \dots}(t)$ are those of the "target system" in dynamical state i.e. composed at an arbitrary time $t < 0$.

Instead of performing the usual perturbation approximation Eqs/4/ will be applied directly to our less general case. The reason of this step lies in the fact that the perturbation approximation converges only for small enough times t of interaction, namely, for $t < \hbar / \max |H_{q|q'}|$, denoting by $H_{q|q'}$ the matrix elements appearing in Eqs/4/. In the case of simple enough problems Eqs/4/ can be solved without making use of iteration and it turns out by comparison that the iteration may converge but poorly if the above condition does not hold. It seems therefore that when using the perturbation approximation up to limited order one can be informed only about the early embryonic stages of the excitation process.

Another advantage of the procedure to be described is that for the simplified system of differential equations the initial conditions can be specified easily and in a quite natural way. /See 2. 4/.

The matrix elements in Eqs/4/ differ from zero only if for one particular frequency ω_k , $n'_k = n_k \pm 1$ while $n'_i = n_i$ / $i \neq k$ / for the rest.

Using the notation

$$n_k B_{q|q'}^{\pm} = (i\hbar)^{-1} \langle n_1 n_2 \dots n_k \dots, \beta_0 \beta_1 \dots / H_{int} / n_1 n_2 \dots n_k \mp 1 \dots, \beta'_0 \beta'_1 \dots \rangle \quad /6/$$

Eqs/4/ become

$$\begin{aligned} \dot{c}_{n_1 n_2 \dots, \beta_0 \beta_1 \dots} = & \sum_k \sum_q \left[n_k B_{q|q'}^{+} e^{i(\omega_{qq'} + \omega_k)t} c_{n_1 n_2 \dots n_k - 1 \dots, q'} + \right. \\ & \left. + n_k B_{q|q'}^{-} e^{i(\omega_{qq'} - \omega_k)t} c_{n_1 n_2 \dots n_k + 1 \dots, q'} \right] \quad /7/ \end{aligned}$$

where, as above, q is a symbol for a specific set of quantum numbers $\beta_0, \beta_1, \dots, \beta_j, \dots$ and $\sum_{q'}$ is equivalent to $\sum_{\beta'_0} \sum_{\beta'_1} \dots$.

Let's assume that the transition frequencies between the various internal states $|\beta\rangle$ differ from each other considerably and that the radiation field consists of quanta with frequencies close to the transition frequencies. Then in Eqs/7/ terms can be found the exponential factor of which varies quite slowly with time. This occurs for those sets $q'(+k)$ and $q'(-k)$ at which

$$\omega_{qq'(+k)} + \omega_k = \Omega_{qk}^+ \ll \omega_k \quad \text{and} \quad \omega_{qq'(-k)} - \omega_k = \Omega_{qk}^- \ll \omega_k,$$

respectively. There can be more than one set equivalent to e.g. $q(+k)$ in this sense and they can be formed by arbitrary changes of indices of the primed β 's in Eq/5b/. Also the matrix elements /6/ are the same for all equivalent sets since only quantum-exchange interaction is allowed. Therefore

$$\begin{aligned} \dot{c}_{n_1 n_2 \dots, q} = & \sum_k \left\{ n_k B_{q|q(+k)}^+ e^{i\Omega_{qk}^+ t} \sum_{q'(+k)} c_{n_1 n_2 \dots n_k - 1 \dots, q'(+k)} + \right. \\ & \left. + n_k B_{q|q(-k)}^- e^{i\Omega_{qk}^- t} \sum_{q'(-k)} c_{n_1 n_2 \dots n_k + 1 \dots, q'(-k)} \right\} + \\ & + \text{terms of higher frequency} \end{aligned} \quad /8/$$

can be written, the summations being performed for all equivalent sets $q'(+k)$ and $q'(-k)$, respectively.

Assuming now that the duration t of the interaction cannot be defined quite sharply, the finer details on the time-dependence of the amplitudes $c_{n_1 n_2 \dots, q}(t)$ are expected to be averaged out so that only components of lowest frequencies are retained. From now on the time t is chosen so as to agree with the average flight-time of the projectiles.

Another point to be stressed is that the functions $c_{n_1 n_2 \dots, q}(t)$ as mathematically correct solutions of the problems drawn up originally in Eqs/1/-/3/ may have discontinuities. In such cases Eq/7/ cannot be solved. To overcome this difficulty one may introduce new functions in place of $c(t)$'s defined by

$$u_{n_1 n_2 \dots, q}(t) = \int_0^t c_{n_1 n_2 \dots, q}(t') dt' \quad /9/$$

They are free from discontinuities even if the $c(t)$'s have and can be introduced by integrating Eqs/8/. This is especially simple for or close to resonance and the resulting system of equations in this case, by dropping the high-frequency terms, is

$$\dot{U}_{n_1 n_2 \dots} = \sum_k \left[n_k B_{q|q(+k)}^+ \sum_{q'(+k)} U_{n_1 n_2 \dots n_k - 1 \dots, q'(+k)} + n_k B_{q|q(-k)}^- \sum_{q'(-k)} U_{n_1 n_2 \dots n_2 + 1 \dots, q'(-k)} \right] + c_{n_1 n_2 \dots, q}(0) \quad /10/$$

The amplitude to the superposition /1/ as determined by the set of equations /10/ and Eq/9/ are complete in the sense that

$$\sum_{n_1} \sum_{n_2} \dots \sum_{\beta_0} \sum_{\beta_1} \dots |c_{n_1 n_2 \dots, \beta_0 \beta_1 \dots}(t)|^2 = 1 \quad /11/$$

at any time t if the initial amplitudes $c_{n_1 n_2 \dots, \beta_0 \beta_1 \dots}(0)$ are chosen accordingly. /It is worth while to mention that this method, when allowing off-resonance frequencies too, can be applied successfully to the treatment of attenuation and broadening of absorption lines./

2.2. In the most simple case the radiation field consists of n quanta of frequency $\omega \approx \omega_{10}$, ω_{10} being the transition frequency between e.g. the first internal excited state $/\beta = 1/$ and the ground state $/\beta = 0/$ of the particle. Apart from the projectile no other particle is present in the cavity.

An initial condition can be that the particle is in its excited state before entering the cavity, i.e. $c_{n', \beta'}(0) = \delta_{nn'} \delta_{1\beta'}$. Eqs/10/ applied to this problem are

$$\dot{U}_{n+1, 0} = n+1 B_{0|1}^+ U_{n, 1} \quad ; \quad \dot{U}_{n, 1} = n B_{1|0}^- U_{n+1, 0} + 1 \quad /10a/$$

and $\dot{U}_{n', \beta'} = 0$ for all other pairs of n', β'

The solutions for the amplitudes $c_{n', \beta'}(t)$ are as follows

$$c_{n+1, 0}(t) \equiv \dot{U}_{n+1, 0} = -i \left(\hbar \Omega_n \right)^{-1} n+1 H_{0|1}^+ \sin \Omega_n t$$

$$c_{n, 1}(t) \equiv \dot{U}_{n, 1} = \cos \Omega_n t \quad /12/$$

and $c_{n', \beta'}(t) \equiv 0$, for all other pairs of n', β' .

In Eq/12/

$$n^H_{\beta|\beta'}^{\pm} = i\hbar_n B_{\beta|\beta'}^{\pm} = \langle n, \beta | H_{int} | n\pm 1, \beta' \rangle \quad /13/$$

and

$$\Omega_n^2 = - n B_{1|0}^{-} \cdot n+1 B_{0|1}^{+} = |n^H_{1|0}^{-}|^2 / \hbar^2 \quad /14/$$

is the square of the state-flipping frequency.

The probability of finding the projectile in its ground state and excited state, respectively, after the cavity has been left is

$$|c_{n+1,0}(t)|^2 = \sin^2 \Omega_n t \quad ; \quad |c_{n,1}(t)|^2 = \cos^2 \Omega_n t \quad /15/$$

as a function of the flight-time t .

In order to calculate the matrix-element /13/ appearing in the expression /14/ of the state-flipping frequency the interaction Hamiltonian should be written in explicit form. This is

$$H_{int} = - \frac{1}{c} \sum_j \int_{V_j} \underline{j}_j \underline{A} dv = - \sum_j \sum_{\underline{k}} \left(\frac{8\pi\hbar}{V\omega} \right)^{1/2} \left[a \int_V \underline{e} \underline{j}_j e^{i\underline{k}\underline{r}'} dv' + a^* \int_V \underline{e} \underline{j}_j e^{-i\underline{k}\underline{r}'} dv' \right] /16/$$

for a linearly polarized radiation field in the cavity of volume V . \underline{e} is the polarization vector and $\underline{k} = \underline{e}\omega/2\pi c$ is the wave-vector. The operators a and a^* are defined by the relations

$$a|n\rangle = \sqrt{n}|n-1\rangle \quad ; \quad a^*|n\rangle = \sqrt{n+1}|n+1\rangle$$

If the particle is of simple enough internal structure the current operator \underline{j}_j can be written as $\underline{j}_j = -i\hbar(e/M)\delta(\underline{r}_j - \underline{r}')\nabla_{\underline{r}_j}$ where the operator $\nabla_{\underline{r}_j}$ acts on the wave-function of the state $|\beta_j\rangle$ only. e/M is the charge-to-mass ratio of the electron if the particle in question is a hydrogen atom. Then the matrix-element /13/ can be written as

$$n^H_{\beta|\beta'}^{-} = \frac{ie\hbar}{M} \left[\frac{8\pi\hbar(n+1)}{V\omega} \right]^{1/2} \langle \beta | \underline{e} \nabla_{\underline{r}} \cos \underline{k}\underline{r} | \beta' \rangle \approx \quad /17/$$

$$\approx -i \left[\frac{8\pi\hbar\omega(n+1)}{V} \right]^{1/2} D_{\beta\beta'} \quad /18/$$

the latter expression concerning dipole-approximation, with the dipole matrix-element $D_{\beta\beta'} = e \langle \beta | \underline{r}_e | \beta' \rangle$.

The final expression for the state-flipping frequency, making use of Eq/18/, is as follows

$$\Omega_n = \frac{1}{\hbar} \left[\frac{8\pi\hbar\omega(n+1)}{v} \right]^{1/2} |D_{10}| \quad /19/$$

The solutions /12/ satisfy Eqs/8/ to a good approximation except region: around

$$t_v = v\pi/\Omega_n \quad /v=0,1,2,\dots/ \quad /20/$$

but which are narrow enough under certain physical conditions. The proof goes as follows.

Introducing by integration the functions $u_{n,\beta}$ defined by Eq/9/ into Eqs/8/ but keeping now the terms of higher frequency, one can find an upper limit for the contributions of the h.f. terms since for any pair of n, β' , $|c_{n,\beta'}(t)| \leq 1$ should be. Assuming the amplitudes /12/ as approximately good solutions, the contributions due to the h.f. terms may upset the equality at the zeros of $U_{n+1,0}(t)$ and $U_{n,1}(t)$, respectively, i.e. at times given by /20/.

Also the regions around t_v , where the approximation may break down can be estimated in the same way with the following result

$$\begin{aligned} \text{around } t = (2v+1)\pi/\Omega_n, \quad \Delta t \leq 4\omega^{-1} \sum_{\beta} |D_{\beta 0}| / |D_{10}| \\ \text{around } t = 2v\pi/\Omega_n, \quad \Delta t \leq \left[(8/\Omega_n \omega) \sum_{\beta} |D_{\beta 1}| / |D_{10}| \right]^{1/2} \end{aligned} \quad /21/$$

If there are no exceedingly high probabilities for cross-over transitions from highly excited states the sum of the relative matrix-elements can be estimated as being in the order of unity. In this case the relative extensions of the regions where the approximation fails to work is in the order of

$$\Delta t/T \approx \begin{cases} \Omega_n/\omega & \text{for } t = (2v+1)\pi/\Omega_n \\ (\Omega_n/\omega)^{1/2} & \text{for } t = 2v\pi/\Omega_n \end{cases} \quad /22/$$

where $T = 2\pi/\Omega_n$. In general, the flipping frequency Ω_n is much less than the transition frequency ω since from /19/

$$\frac{\Omega_n}{\omega} = \frac{|D_{10}|}{h\omega} \left[\frac{8\pi h\omega(n+1)}{v} \right]^{1/2} \quad /23/$$

follows. If $n \gg 1$ then the square-root is equivalent to the classical field-strength \mathcal{E}_0 in the cavity.

The structure of Eqs/8/ and also the above estimations suggest that the true solutions differ from those given by Eqs/10a/ in quickly oscillating terms of moderate amplitude. One can expect therefore that an uncertainty in t would smooth the rapid oscillations so that under realistic physical conditions the approximation may be perhaps even better.

2.3. The model proposed for the estimation of the charge-state flipping frequency in neutron-proton scattering was that the cavity contains one particle in ground state and no quanta while the projectile enters the cavity in its excited state at $t' = 0$. The amplitudes to be considered are as follows

- $c_{0,10}$: no quanta in the cavity, the projectile is in excited state, the other particle in ground state.
- $c_{0,01}$: no quanta in the cavity, the states of the particles are changed respect to the previous case.
- $c_{1,00}$: the cavity contains one quantum and both particles are in ground state.

Applying the approximation outlined in 2.1. one gets for resonance

$$\dot{U}_{0,10} = {}_0B_{11}^- U_{1,00} + c_{0,10} (0) \quad /10b/$$

$$\dot{U}_{0,01} = {}_0B_{11}^- U_{1,00} + c_{0,01} (0)$$

$$\dot{U}_{1,00} = {}_1B_{01}^+ (U_{0,10} + U_{0,01}) + c_{1,00} (0)$$

This set of equations can be solved readily and the amplitudes in this approximation are

$$c_{0,10}(t) \equiv \dot{U}_{0,10} = \frac{1}{2} (1 + \cos \Omega_1 t) \quad /24/$$

$$c_{0,01}(t) \equiv \dot{U}_{0,01} = -\frac{1}{2} (1 - \cos \Omega_1 t)$$

$$c_{1,00}(t) \equiv \dot{U}_{1,00} = -i \left(| {}_0H_{1|0}^- | / \sqrt{2} \right) \sin \Omega_1 t$$

in the case of the initial conditions given above. The state flipping frequency Ω_1 is now

$$\Omega_1 = \sqrt{2} | {}_0H_{1|0}^- | / \hbar \quad /25/$$

The probability that the projectile leaves the cavity in ground state is

$$w(t) = |c_{0,01}(t)|^2 + |c_{1,00}(t)|^2 = 1 - \cos^4 \frac{\Omega_1}{2} t \quad /26/$$

Let's suppose that the projectile crosses the cavity /at rest/ with a relative kinetic energy E , where its path-length is d .

Then

$$\Omega t = \frac{\pi}{2} \alpha \sqrt{2/mc^2} \beta^{-1} \quad /27/$$

$$\approx \frac{\pi}{2} \frac{\alpha}{\sqrt{E'}} \quad , \quad \text{if } \beta = v/c \ll 1 \quad /28/$$

where

$$\alpha = \Omega d (2m)^{1/2} / \pi \quad /29/$$

and

$$\beta(E') = \left\{ 1 - (1 + E'/mc^2)^{-2} \right\}^{1/2} \quad /30/$$

m is the rest-mass of the particles for which $m \gg \hbar\omega/c^2$ is assumed.

For non-relativistic velocities the charge-state flipping contribution to the cross-section will be taken as

$$\sigma_{fl}(E) = K w(E) = K \left(1 - \cos^4 \frac{\pi}{2} \frac{\alpha}{\sqrt{E+\epsilon}} \right) \quad (\beta \ll 1) \quad /31/$$

$$\approx \frac{2K}{\pi} \sin^2 \frac{\pi}{2} \frac{\alpha}{\sqrt{E}} + \text{const} \quad /32/$$

when simulating the finite energy resolution of a measurement by an averaging over intervals of a quarter of a full periode.

The matrix-element appearing in Eq/25/ is given by Eq/18/ for electric dipole transitions. It is reasonable to assume for an estimation that in the case to be investigated $\hbar\omega = m_{\pi}c^2$ where m_{π} is the mass of charged pions and that the interaction volume V is defined by the pion Compton wavelength i.e. by a sphere of radius $\lambda_{\pi c} = \hbar/m_{\pi}c$. Further, we shall assume, that in place of the dipole-matrix-element $|D_{10}|, |D_{10}| = f \cdot d$ can be written where $d = 2\lambda_{\pi c}$ and f is the pion-nucleon coupling constant. By these assumptions one gets for the parameter α_{np}

$$\alpha_{np} = \left[\frac{96}{\pi} mc^2 \left(f^2/\hbar c \right) \right]^{1/2} = 28 \cdot 0 \text{ MeV}^{1/2} \quad /33/$$

where m is the mean nucleon mass and $f^2/\hbar c = 0 \cdot 085$ was substituted for the dimensionless coupling-constant of the pion-nucleon interaction. The upper limit K of the charge-state flipping contribution to the cross section can be estimated as

$$K \approx \lambda_{\pi c}^2 \quad \pi \approx 60 \text{ mb} \quad /34/$$

2.4. The estimation of the charge-state flipping frequency for neutron scattering on deuteron can follow the same line as in the case of n-p scattering. The amplitudes are now $c_{n, \beta_0 \beta_1 \beta_2}(t)$ referring to the charge-state of the particles by the quantum numbers β_j and to the number of quanta present in the cavity by n , respectively. Again, it will be assumed that in the initial state /at $t' = 0$ / the projectile is in excited state $\beta_0 = 1$ / while as for the particles in the cavity $\beta_1 = \beta_2 = 0, n=1$ or, if $n=0, \beta_1 = 1, \beta_2 = 0$, or vice versa.

The probability that the projectile leaves the cavity in ground state can be written as

$$w(t) = |c_{0,011}(t)|^2 + |c_{1,001}(t)|^2 + |c_{1,010}(t)|^2 + |c_{2,000}(t)|^2 \quad /35/$$

The system of equation to be solved is

$$\begin{aligned} \dot{U}_{0,101} &= {}_0B_{2|1}^- (U_{1,001} + U_{1,010} + U_{1,100}) + c_{0,101}(0) \\ \dot{U}_{0,110} &= {}_0B_{2|1}^- (U_{1,001} + U_{1,010} + U_{1,100}) + c_{0,110}(0) \\ \dot{U}_{0,011} &= {}_0B_{2|1}^- (U_{1,001} + U_{1,010} + U_{1,100}) \\ \dot{U}_{1,001} &= {}_1B_{1|0}^- U_{2,000} + {}_1B_{1|2}^+ (U_{0,101} + U_{0,011} + U_{0,110}) \quad /10c/ \\ \dot{U}_{1,010} &= {}_1B_{1|0}^- U_{2,000} + {}_1B_{1|2}^+ (U_{0,101} + U_{0,011} + U_{0,110}) \\ \dot{U}_{1,100} &= {}_1B_{1|0}^- U_{2,000} + {}_1B_{1|2}^+ (U_{0,101} + U_{0,011} + U_{0,110}) + c_{1,100}(0) \\ \dot{U}_{2,000} &= {}_2B_{0|1}^+ (U_{1,001} + U_{1,010} + U_{1,100}) \end{aligned}$$

and the solutions which come into the expression /35/ of the transition probability are as follows.

$$\begin{aligned} c_{0,011}(t) &= 3M \left[\frac{c_1}{3} \sin \Omega_2 t - M^* c_0 (1 - \cos \Omega_2 t) \right] \\ c_{1,001}(t) &= - \left[\frac{c_1}{3} (1 - \cos \Omega_2 t) + M^* c_0 \sin \Omega_2 t \right] \quad /36/ \end{aligned}$$

$$c_{1,010}(t) \equiv c_{1,001}(t)$$

$$c_{2,000}(t) \equiv \frac{{}_2B_{0|1}^+}{{}_0B_{2|1}^-} c_{0,011}(t)$$

where

$$M = {}_0B_{2|1}^- / \Omega_2$$

$$M^* = - {}_1B_{1|2}^+ / \Omega_2$$

$$c_1 = c_{1,100}(0)$$

$$c_0 = c_{0,101}(0) + c_{0,110}(0)$$

and the state flipping frequency Ω_2 is

$$\Omega_2 = \left[3|{}_1H_{1|0}^-|^2 + 9|{}_0H_{2|1}^-|^2 \right]^{1/2} \hbar^{-1} \quad /37/$$

Substituting the amplitudes /36/ into the expression /35/ of $w(t)$ it takes the simple form

$$w(t) = \frac{4}{9} \left[2|c_{1,100}(0)|^2 + |c_{0,101}(0) + c_{0,110}(0)|^2 \right] \sin^2 \frac{\Omega_2}{2} t \quad /38/$$

if

$$|{}_{1H_{1|0}}^-|^2 = 3|{}_{0H_{2|1}}^-|^2 \quad /39/$$

is assumed.

Since the initial amplitude values appearing in Eq/38/ are those of two particles and maximum one quantum in the cavity and one particle being out of it they should be identical with the amplitudes /24/ taken at any arbitrary time after that target-system was formed. Substituting the latter amplitudes one finds that $w(t)$ is in fact independent of when and how the target-system was formed, for the expression appearing in the bracket of Eq /38/ identically equals to unity.

The charge-state flipping contribution to the n-d cross-section can be written therefore as

$$\sigma_{fl}(E) = \frac{4}{9} K' \sin^2 \frac{\pi}{2} \frac{\alpha_{nd}}{\sqrt{E}} \quad /40/$$

for non-relativistic velocities of the projectile.

Making use of Eq /39/ the flipping frequency Ω_2 can be expressed as

$$\Omega_2 = \sqrt{6} |{}_{1H_{1|0}}^-| \hbar^{-1} \approx \left(6 \frac{v_{np}}{v_{nd}} \right)^{1/2} \frac{r_{nd}}{r_{np}} \Omega_1 \quad /41/$$

if Eq /18/ is assumed. Since $\alpha \sim \Omega d$, the parameter α_{nd} can be given in terms of α_{np} as

$$\alpha_{nd} \approx \left(6 \frac{r_{nd}}{r_{np}} \right)^{1/2} \alpha_{np} \quad /42/$$

For a rough estimation $r_{nd}/r_{np} \approx 1.5^{1/3}$ will be assumed and one finds a lower limit for α_{nd} as $\alpha_{nd} \geq 2.6 \alpha_{np} = 73 \text{ MeV}^{1/2}$ when making use of the parameter value $\alpha_{np} = 28 \text{ MeV}^{1/2}$ as found above.

3 §. Analysis of the experimental data

A relatively large number of experimental data on the total cross-section of neutron-proton scattering is available from the literature [4 - 28] , for neutron energies ranging up from about 1 MeV. Usually, they were measured with a considerable accuracy as several percent or, at few isolated energies, even below one percent. Unfortunately, however, in many cases no error was given, especially for data below 14 MeV which though were rather important from our point of view. Since the number of these low-energy data still reaches as much as 100 that drawback can be compensated in a considerable extent by applying a simple statistical treatment.

For neutron energies where s-wave scattering is expected to predominate the energy-dependence of the total cross-section of n-p scattering $\sigma_{np}(E)$ is given by the shape-independent effective range theory. This leads to the following well known expression [2].

$$\bar{\sigma}_{np}(k^2) = \frac{3}{4} \cdot \frac{4\pi}{k^2 + \left[R^{-1} - \frac{1}{2} r_t (k^2 + R^{-2}) \right]^2} + \frac{1}{4} \cdot \frac{4\pi}{k^2 + \left(a_s^{-1} - \frac{1}{2} r_s k^2 \right)^2} \quad /43/$$

which is a smooth function of the neutron kinetic-energy, k being the wave-number of the relative motion. The parameters appearing in Eq/43/ are the deuteron radius R , the singlet scattering length a_s , the singlet and triplet effective ranges r_s and r_t , respectively. It is generally assumed that Eq/43/ is the right expression for the low-energy/ $E < 8$ MeV/ n-p scattering when using the parameter values

$$R = 4.316 \pm 0.002 \text{ fm} , \quad a_s = -23.678 \pm 0.028 \text{ fm} ,$$

$$r_s = 2.51 \pm 0.11 \text{ fm} \quad \text{and} \quad r_t = 1.726 \pm 0.014 \text{ fm},$$

as deduced from a recent comparison [3] with experiments, including 8 selected data on $\bar{\sigma}_{np}$ below 5 MeV.

It is also agreed that the angular distribution of n-p scattering is isotropic in center-of-mass system, below 8 MeV /all our energy data referring to laboratory energies/, i.e. the effect of higher partial waves is negligible [3] in this energy-region.

Provided the charge-state flipping phenomenon exists in this case too, it should modulate the energy-dependence of the total cross-section

$\sigma_{np}(E)$ respect to the smooth function given by Eq/43/. Its maximum contribution K was estimated as being about 60 mb while the sequence of the maxima and minima should follow the rules $E_v^{\max} = [\alpha/(2v+1)]^2$ and $E_v^{\min} = (\alpha/2v)^2$, ($v=0,1,2\dots$), respectively, for non-relativistic neutron velocities, as following from Eqs/31/ or /32/. The parameter α was estimated to be about $28 \text{ MeV}^{1/2}$.

As regards the higher energies, Eq/43/ can be considered only as some smooth background-function and will be used in this sense.

From the cross-section data the corresponding calculated values $\bar{\sigma}_{np}(E)$ given by Eq/43/ were subtracted. For neutron energies below 120 MeV these reduced cross-section data were grouped into reasonably small energy intervals so that in the mean six data contributed to each point. As error the standard deviation was assumed for each group. In Table 1. the data so calculated are given. In the first column the average energy of the groups, in the second and third the average reduced cross-section is presented together with the error assumed. The fourth column presents the corresponding references. The second part of Table 1. is constructed in a similar way but with data regrouped.

In Fig. 1 the results are seen, with full and open circles, respectively, for the average values given in the two parts of Table 1. The reduced data for neutron energies above 120 MeV are plotted directly and the errors shown are those given by the authors.

The data so presented seem to show fluctuations of some regular sequence and of amplitudes in the order of magnitude as expected. Below 2 MeV, however, the number of data is too low to show any particular structure.

Table 1.

Mean deviations from Eq/43/ of total cross-section data groups for neutron-proton scattering. The data were taken from references as indicated. In the first two part of the Table \bar{E} is the average neutron energy for a group and the errors are standard-deviations. The second part is compiled using the same but regrouped data of the first part. The third part consists of single measured data with energies and cross-section errors as given by the authors.

I.

II.

\bar{E} /MeV/	$\langle\sigma_{np}-\bar{\sigma}_{np}\rangle$ /mb/	$\Delta\langle\sigma_{np}-\bar{\sigma}_{np}\rangle$ /mb/	References	\bar{E} /MeV/	$\langle\sigma_{np}-\bar{\sigma}_{np}\rangle$ /mb/	$\Delta\langle\sigma_{np}-\bar{\sigma}_{np}\rangle$ /mb/	References
1.10	20.8	46.5	4.,5.,7.	1.22	13.6	28.0	4.,5.,6.,7.
1.56	-13.5	22.8	4.,5.,7.	2.20	-18.0	24.2	4.
1.43	12.0	11.0	4.,5.,8.,9.	2.57	16.7	23.0	4.,5.,8.,9.
2.68	13.0	29.6	4.,9.	2.85	-5.0	23.3	4.,9.,10.
3.05	-6.0	16.8	4.,10.,11.	3.27	0.3	8.9	10.,11.
3.82	-65.5	22.7	4.,9.,10.,12.	3.60	-9.0	19.5	4.,9.,10.
4.57	-22.5	23.2	4.,10.,13.	4.12	-95.1	24.0	4.,9.,10.,12.
4.97	-7.0	12.3	4.,9.,10.	4.76	-5.0	18.8	4.,9.,10.,13.
5.42	-22.5	22.1	9.,10.	5.21	-26.2	23.8	4.,10.
5.88	-55.5	31.2	4.,9.,10.	5.66	-14.0	10.2	9.,10.
6.37	2.5	15.1	9.,10.	6.15	-32.6	28.0	4.,9.,10.
7.12	10.0	13.2	10.	6.70	-21.7	6.0	10.
7.87	2.8	15.4	9.,10.	7.28	23.3	9.3	10.
9.27	-21.2	20.0	9.,10.	7.77	17.5	7.5	10.
10.60	-34.2	21.2	4.,9.,10.	8.38	-13.7	21.1	9.,10.
12.54	8.8	26.0	9.,10.,12.	9.43	-31.7	24.1	9.,10.
13.97	24.1	8.7	12.,14.,-20.	10.52	-57.5	24.0	4.,9.,10.
14.90	7.0	10.7	9.,14.,16.,18.,21.	12.05	8.2	21.2	9.,10.,12.
16.53	12.5	12.4	9.,18.,21.	14.00	12.0	8.3	9.,12.,14-20.
18.69	12.3	4.0	9.,18.,21-23.	15.55	-7.5	16.0	9.,16.,18.,21.
21.32	1.2	6.3	9.,21.	17.12	22.2	6.8	9.,18.,21.
24.89	5.5	3.8	9.,21.,24.	19.53	12.4	3.9	9.,21.-23.
29.22	-2.4	2.7	21.	22.81	-0.1	6.0	9.,21.
34.09	-0.1	5.3	21.	26.71	2.0	3.7	21.,24.
39.89	2.0	5.2	14.,21.,25.	31.28	2.2	4.5	21.
46.6	10.7	4.8	14.,21.	36.98	-1.9	3.2	21.,25.
53.6	4.32	2.4	21.	43.0	-0.80	6.5	14.,21.
61.6	7.47	2.0	21.,25.	49.3	8.02	5.4	14.,21.
69.0	8.20	1.1	21.	57.7	7.10	1.5	21.
81.8	10.78	0.75	14.,21.	65.4	8.57	1.7	21.,25.
93.2	12.98	0.72	14.,21.,25.,27.	75.4	10.36	2.1	21.
107.2	17.03	2.4	21.,27.,28.	90.0	11.87	0.77	14.,21.,25.,27.
				100.7	15.07	2.0	21.,27.,28.
\bar{E} /MeV/	$\langle\sigma_{np}-\bar{\sigma}_{np}\rangle$ mb	$\Delta\langle\sigma_{np}-\bar{\sigma}_{np}\rangle$ mb	Reference	\bar{E} /MeV/	$\langle\sigma_{np}-\bar{\sigma}_{np}\rangle$ mb	$\Delta\langle\sigma_{np}-\bar{\sigma}_{np}\rangle$ mb	Reference
126	16.9	1.8	25.	410	28.6	1.3	} 14.
140	15.0	5.6	28.	500	31.5	2.0	
153	17.4	1.2	25.	590	33.4	2.0	
156	22.5	8.3	28.	630	34.7	4.0	
160	24.2	2.6	14.	805	27.1		
169	24.2	1.6	14.	1060	26.9		
180	21.5	12.0	28.	1260	32.4		
220	25.8	1.5	28.	1400	42.4	1.8	
270	27.0	1.5	14.	1450	32.5		
280	23.0	3.0	14.	2020	35.2		
380	34.0	4.0	14.	2600	32.4		
390	28.0	2.0	14.				

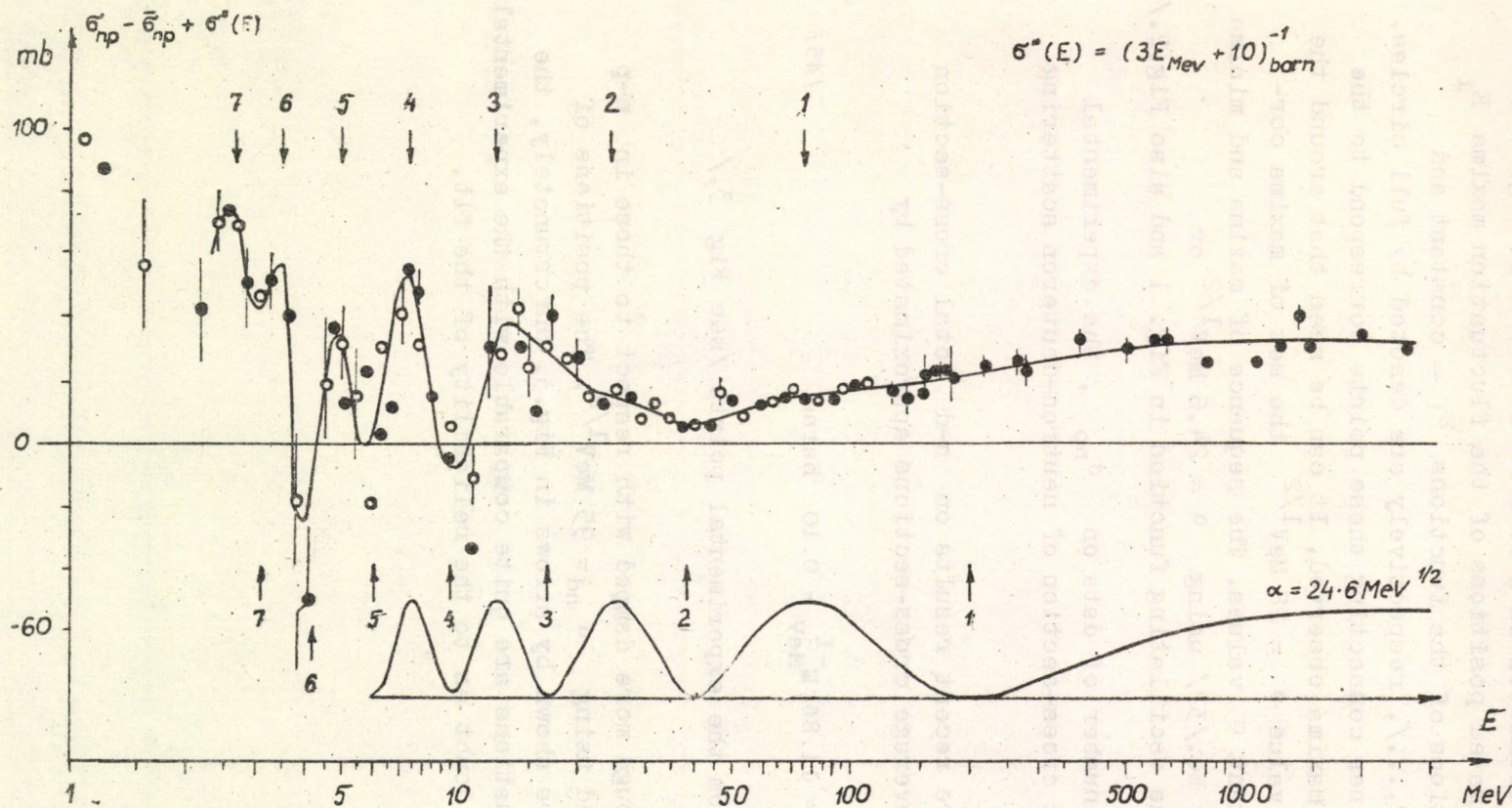


Fig.1.

Mean deviations from a smooth function of neutron energy of total cross-section data groups, for neutron-proton scattering. The data groups are those given in Table 1. and the function is Eq/43/ corrected with $\sigma^s(E) = (3E_{MeV} + 10)^{-1}$ barns, to rise the deviations possibly to the positive region. The two sets of data groups corresponding to the parts I. and II. of Table 1. are indicated with open and full circles, respectively. The arrows show the expected positions of maxima and minima for $\alpha = 24.6 \text{ MeV}^{1/2}$ and $\epsilon = 0$.

The sequence of the observed maxima corresponds well to α values which are close to that estimated in § 2. This is shown in Fig.2. On the energy axis the estimated positions of the fluctuation maxima E_i are given. The intersections of the functions $E_i = \text{constant}$ and $\alpha = (2v+1) \sqrt{E}$ / $v=0,1,2,\dots$ /, respectively are denoted by full circles. The shortest straight lines connecting these points correspond to the closest sequence of the maxima observed. It can be seen that around the theoretically estimated value $\alpha = 28 \text{ MeV}^{1/2}$ the set of maxima corresponds to nearly constant α values. The sequence of maxima and minima can be best described by Eq./32/ using $\alpha = 24.6 \text{ MeV}^{1/2}$ or $\alpha = 28.7 \text{ MeV}^{1/2}$ /see the oscillating function in Fig. 1 and also Fig.2./.

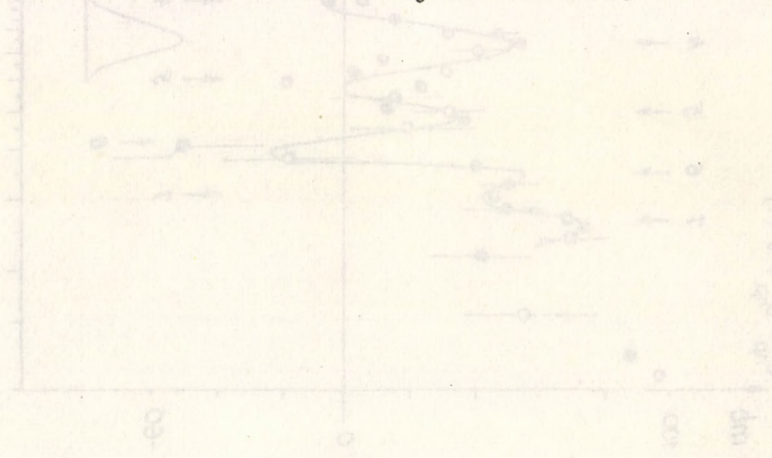
As compared with the number of data on σ_{np} , the experimental information on the total cross-section of neutron-deuteron scattering is rather scarce.

Investigating the more recent results on n-d total cross-section [29] in a similar way, average cross-sections approximated by

$$\bar{\sigma}_{nd}(E) = 11.86 E_{\text{MeV}}^{-1} - 0.10 \text{ barns} \quad /45/$$

have been subtracted from the experimental points /see Fig. 3./

The fluctuations, though more damped with respect to those in n-p scattering, can be fitted using $\alpha_{nd} = 95 \text{ MeV}^{1/2}$. The positions of the calculated maxima are shown by arrows in Fig.3. Unfortunately, the amplitudes of the fluctuations are quite comparable with the experimental errors which casts some doubt as to the reliability of the fit.



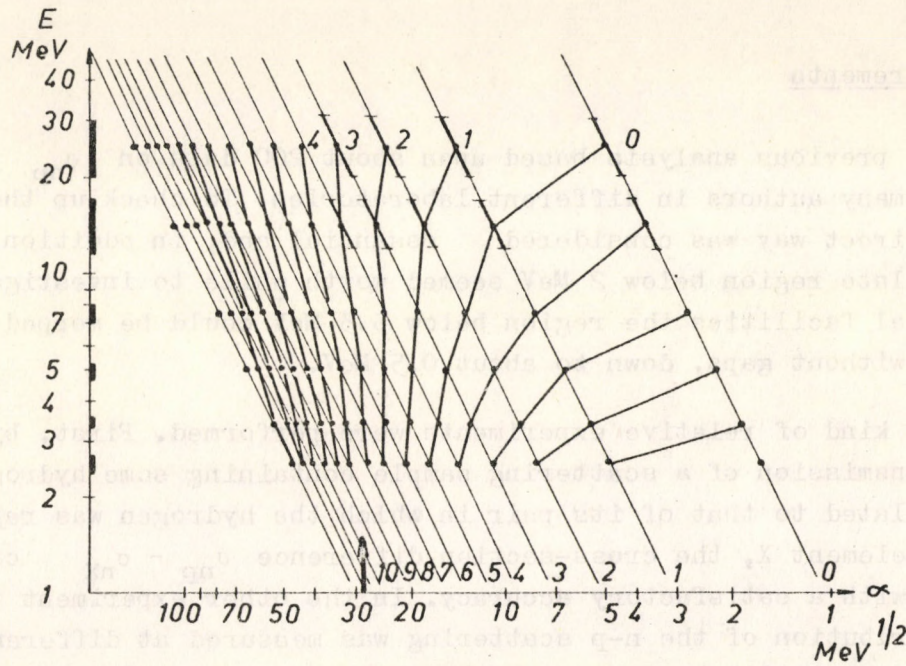


Fig. 2

Diagram showing the right sequence of fluctuation maxima for different α values close to the theoretically estimated $28 \text{ MeV}^{1/2}$ as shown by arrow. For details see text

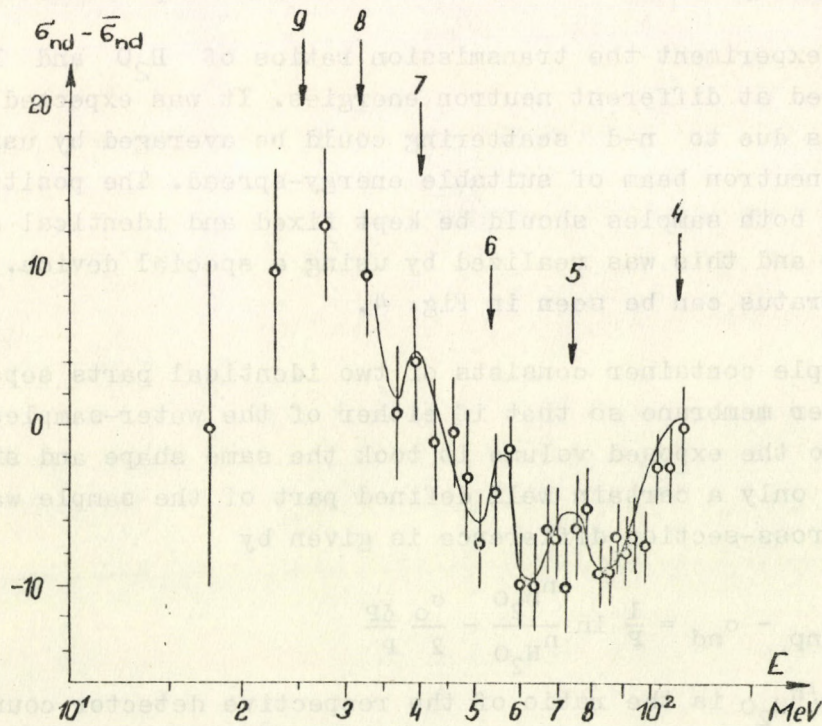


Fig. 3

The deviations of total cross-section data /from ref.29./ of $n - d$ scattering from a smooth function of energy as indicated in the text. The arrows show the positions of the maxima if $\alpha_{nd} = 95 \text{ MeV}^{1/2}$ is assumed

4 §. Measurements

The previous analysis based upon about 200 data on σ_{np} measured, though, by many authors in different laboratories. To check up the results in a more direct way was considered essential and, in addition, the rather desolate region below 2 MeV seemed worth while to investigate. With our technical facilities the region below 5.3 MeV could be mopped up, though not without gaps, down to about 0,5 MeV.

Two kind of relative experiments were performed. First, by measuring the transmission of a scattering sample containing some hydrogen-compound as related to that of its pair in which the hydrogen was replaced by a suitable element X, the cross-section difference $\sigma_{np} - \sigma_{nX}$ can be determined with a satisfactory accuracy. In the other experiment the proton energy distribution of the n-p scattering was measured at different neutron energies and from that the energy-dependence of the relative differential cross-section could be deduced.

4.1. The relative-transmission measurement has been made possible by the suggestion that the fluctuations, if exist, are of more damped and of higher frequency in the case of n-d than for n-p scattering.

In our experiment the transmission ratios of H_2O and D_2O samples were measured at different neutron energies. It was expected that the fluctuations due to n-d scattering could be averaged by using a bombarding neutron beam of suitable energy-spread. The position, shape and size of both samples should be kept fixed and identical as exactly as possible and this was realized by using a special device. The scheme of the apparatus can be seen in Fig. 4.

The sample container consists of two identical parts separated by a thin rubber membrane so that if either of the water-samples was pressed into the exposed volume it took the same shape and size. In such a way, only a certain well defined part of the sample was changed. The total cross-section difference is given by

$$\sigma_{np} - \sigma_{nd} = \frac{1}{P} \ln \frac{n_{D_2O}}{n_{H_2O}} - \frac{\sigma_O}{2} \frac{\delta P}{P} \quad /45/$$

where n_{D_2O}/n_{H_2O} is the ratio of the respective detector counts, background subtracted, measured for equal monitor counts. $P = 2\rho\ell$, ρ being the number of water molecules per unit volume and ℓ is the length of the sample region which is exchanged /see Fig.4./. σ_O is the total cross-section of the oxygen nucleus at the same energy. δP expresses

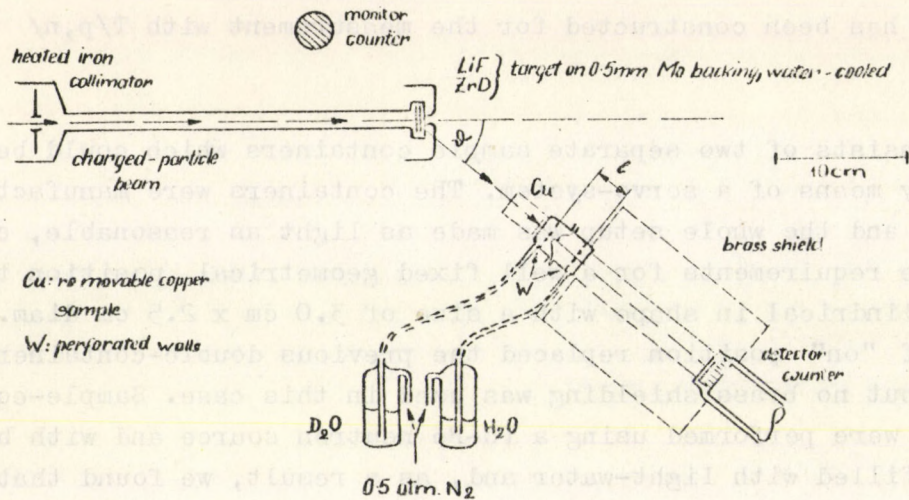


Fig. 4

The scheme of the apparatus used for the measurement of the total cross-section difference $\sigma_{np} - \sigma_{nd}$.

the asymmetry in the samples due mainly to the small difference between σ_{H_2O} and σ_{D_2O} their ratio being $\sigma_{D_2O}/\sigma_{H_2O} = 0.996$ at room temperature. The contribution of this asymmetry term in Eq./45/ was calculated as less than 16 mb and 30 mb for the neutron energy regions $0.8\text{MeV} < E < 5.3\text{MeV}$ and $0.4\text{MeV} < E < 0.5\text{MeV}$, respectively.

Our monoenergetic neutron-sources were the following reactions: ${}^7\text{Li}/p,n/{}^7\text{Be}$ /0.4 MeV $< E < 0.5$ MeV/, $\text{T}/p,n/{}^3\text{He}$ /0.8 MeV $< E < 1.6$ MeV/ and $\text{D}/d,n/{}^3\text{He}$ /2.5 MeV $< E < 5.3$ MeV/. Moderately thin targets as $\text{LiF}/150 \mu\text{g}/\text{cm}^2/$, $\text{Ti-D}/0.5$ and $1.0 \text{ mg}/\text{cm}^2/$ and $\text{Ti-T}/0.3$ and $1.2 \text{ mg}/\text{cm}^2/$ were used, all types on 0.3 mm thick Mo backing. The targets were bombarded with a beam current of about 1 - 2 μA . To have a stable enough neutron yield intensive target-cooling was necessary. The energy of the charged particles was kept constant within ± 2 keV and the neutron energy was varied by changing the angle ϑ_n .

In order to determine the background the transmission of an additional Cu sample /3.0 cm x 2.5 cm diam./ was also measured at each energy and the cross-section data as given by ref 4./ were assumed.

In the case of this setup the background could not be depressed below 15 - 30 % /depending on the neutron energy/ and we found that originating mainly from the flanges of the sample container. Fortunately, however, the background correction did not have too much effect in the region $2.5 \text{ MeV} < E < 5.3 \text{ MeV}$ since here the average cross-section $\bar{\sigma}_{np}$ and $\bar{\sigma}_{nd}$ hardly differ by 50 mb /see ref 4./.. Nevertheless, an

other setup has been constructed for the measurement with T/p,n/ neutrons.

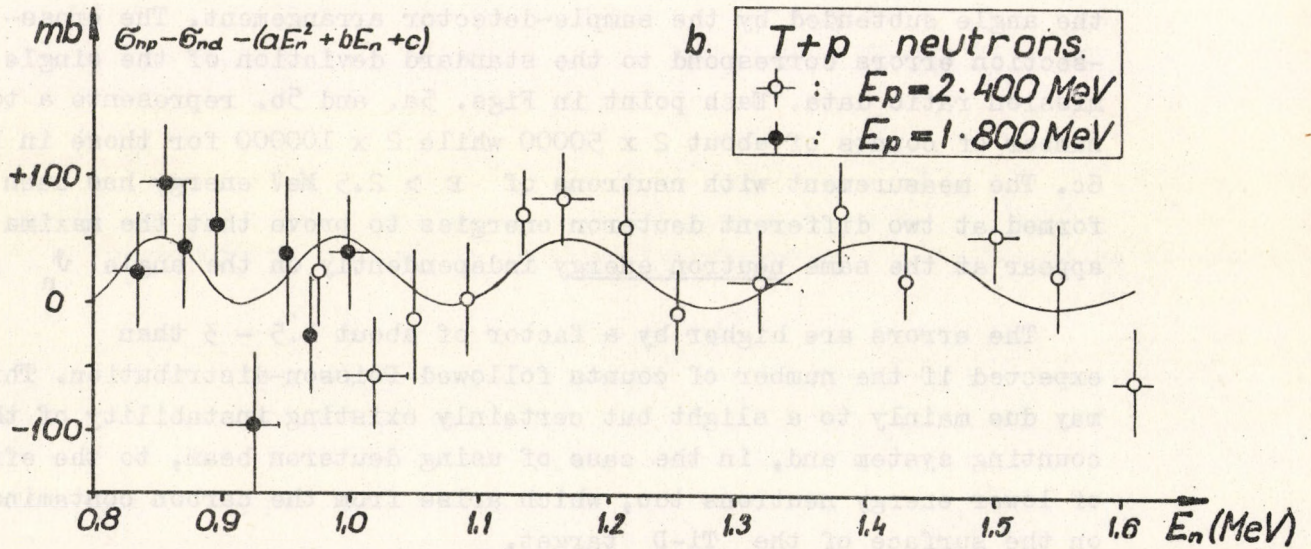
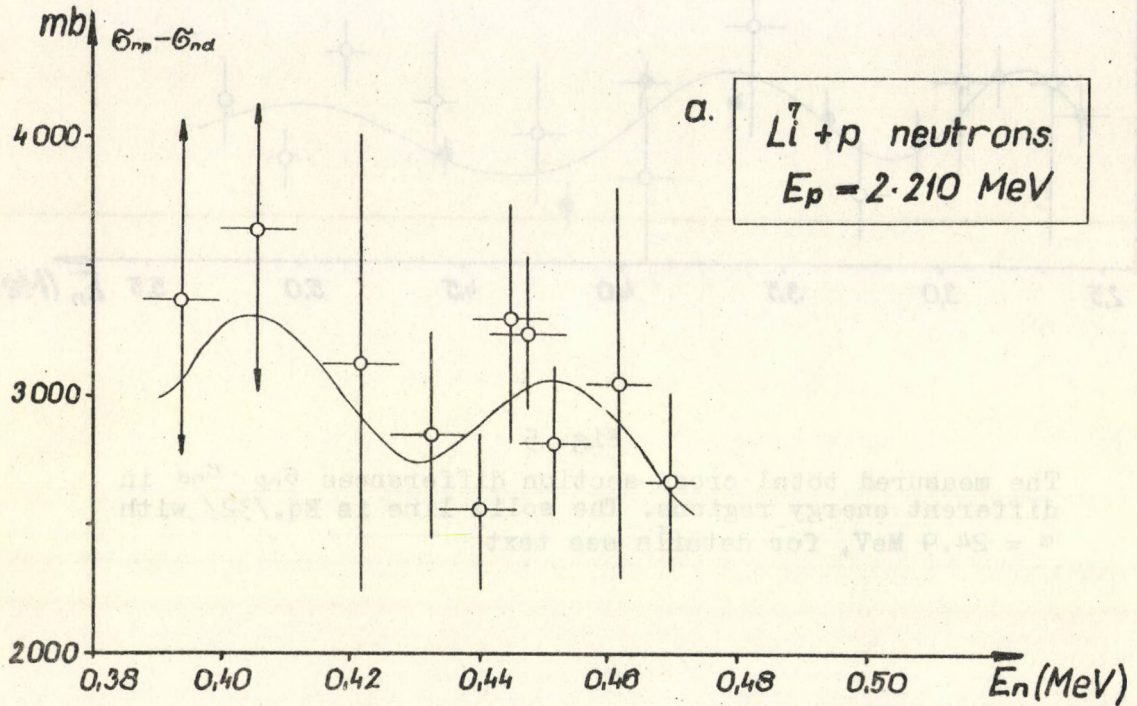
This consists of two separate sample containers which could be exchanged by means of a servo-system. The containers were manufactured from copper and the whole setup was made as light as reasonable, considering the requirements for a well fixed geometrical position too. They are cylindrical in shape with a size of 3.0 cm x 2.5 cm diam. A container of "on" position replaced the previous double-container seen in Fig. 4. but no brass shielding was used in this case. Sample-equivalence tests were performed using a Po-Be neutron source and with both containers filled with light-water and, as a result, we found that the transmission ratio so measured was 0.6 % off the optimal value. This deviation, however, could be tolerated.

The background of this setup was controlled carefully during the course of the measurements and it was found to be less than 5 %.

Both the monitor and the detector were scintillation counters with similar Emmerich-type phosphors [30] and selected photomultipliers to give approximately identical responses at the same anod-voltage. In order to improve the reliability of such a counting system both photomultipliers were fed from one power-supply and the counting periods /for one sample/ were kept as short as 60 - 150 seconds. From the point of view of counting stability the use of scintillation counters with Emmerich-phosphors is not very favourable. Still, they were preferred because of their nearly absolute insensitivity to any γ -radiation which clearly was an important point of this measurement.

Since we did not aim at an absolute cross-section determination neither multiple-scattering nor in-scattering corrections were necessary. These effects may only damp the fluctuations and because of the relatively small size of the samples no serious distortion was expected.

The results can be seen in Figs 5a-5c. for the three energy regions investigated. Each point corresponds to the cross-section difference



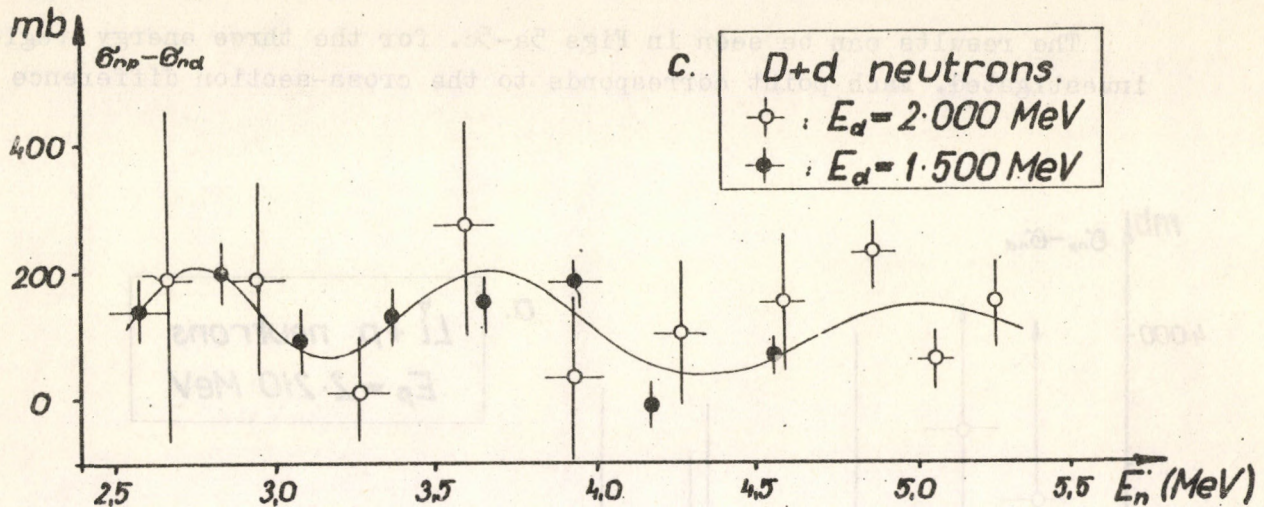


Fig. 5

The measured total cross-section differences $\sigma_{np} - \sigma_{nd}$ in different energy regions. The solid line is Eq./32/ with $\alpha = 24.9$ MeV, for details see text

$\sigma_{np} - \sigma_{nd}$ as calculated from the mean-value of the transmission-ratios measured at an energy E . The energy-errors were calculated from reaction kinematics, taking into account the target-thickness and the angle subtended by the sample-detector arrangement. The cross-section errors correspond to the standard deviation of the single transmission ratio data. Each point in Figs. 5a. and 5b. represents a total number of counts of about 2×50000 while 2×100000 for those in Fig. 6c. The measurement with neutrons of $E > 2.5$ MeV energy has been performed at two different deuteron energies to prove that the maxima appear at the same neutron energy independently on the angle ϑ_n .

The errors are higher by a factor of about 1.5 - 3 than expected if the number of counts followed Poisson-distribution. This may be due mainly to a slight but certainly existing instability of the counting system and, in the case of using deuteron beam, to the effect of lower energy neutrons too, which arise from the carbon contamination on the surface of the Ti-D target.

Table 2.

The measured total cross-section differences $\sigma_{\text{meas}} = \sigma_{\text{np}} - \sigma_{\text{nd}}$ for different neutron energies E . The energy errors are calculated on the base of reaction kinematics, the cross-section errors are standard deviations

E/keV/	$\Delta E/\text{keV}/$	$\sigma/\text{mb}/$	$\Delta \sigma/\text{mb}/$	E/MeV/	$\Delta E/\text{keV}/$	$\sigma/\text{mb}/$	$\Delta \sigma/\text{mb}/$
0.394	6	3370	2230	1.255	25	891	32
0.406	6	3640	1330	1.320	25	832	38
0.422	6	3130	900	1.380	20	828	35
0.433	6	2840	410	1.430	20	729	27
0.440	6	2560	320	1.500	20	716	34
0.445	6	3310	440	1.570	15	651	32
0.448	6	3260	300	1.610	15	553	39
0.452	6	2820	290				
0.462	5	3060	760	2.53	100	140	48
0.470	4	2670	350	2.67	90	189	256
				2.83	100	201	50
0.835	20	1743	47	2.95	100	193	152
0.855	20	1764	45	3.09	100	93	45
0.868	20	1682	49	3.27	100	10	84
0.895	20	1632	38	3.37	120	129	45
0.925	20	1403	57	3.60	110	272	178
0.950	20	1478	59	3.65	110	150	45
0.970	20	1373	47	3.93	110	31	126
0.975	25	1411	46	3.94	100	185	32
1.000	15	1373	44	4.18	100	- 9	35
1.020	25	1238	43	4.28	90	103	111
1.050	25	1219	56	4.56	100	69	27
1.090	25	1160	47	4.59	80	148	112
1.135	25	1143	33	4.86	70	231	47
1.165	25	1112	35	5.06	50	60	40
1.215	25	1011	36	5.24	10	153	70

The results support what has been found in § 3. In the energy region 2.5 MeV - 5.3 MeV the maxima and minima coincide with those labelled by 5, 6 and 7 in Fig. 1. Furthermore, the measured data of the three intervals can be fitted with one single function given by Eq /32/ at well determined sharp values of the frequency parameter α . For each interval the parameters a, b, c and k of the function

$$\sigma_{\text{calc}}(E, \alpha) = \sigma_{\text{np}} - \sigma_{\text{nd}} = k \sin^2\left(\frac{\pi\alpha}{2\sqrt{E}}\right) + aE^2 + bE + c \quad /46/$$

have been determined by weighted least square analysis for fixed α values. When assuming a fixed sign /+/ for the amplitude two sharp minima occur /see Fig. 6/ in the function $\chi^2(\alpha)$ defined as

$$\chi^2(\alpha) = \sum_i \frac{1}{(\Delta\sigma_i)^2} [\sigma_{\text{meas}}(E_i) - \sigma_{\text{calc}}(E_i, \alpha)]^2 \quad /47/$$

where i runs over all measured data summarized in Table 2. In Fig. 6 also the probabilities to find a certain value of χ^2 are shown.

The best fitting parameters of Eq. /46/ are given in Table 3. The α values found in this analysis /24.9 MeV^{1/2} and 28.9 MeV^{1/2}/ well agree with those found in § 3. /24.6 MeV^{1/2} and 28.7 MeV^{1/2}/. However, we cannot decide which α value is the true one since χ^2 is practically the same for both. The reason of this peculiar ambiguity may be mathematical, such kind of ambiguity can occur if a finite number of points measured with some uncertainty are to be fitted with a periodical function over a finite interval /even if the points themselves show clear signes of periodicity/. The corresponding frequencies are not necessarily multiples of some basic frequency. Nevertheless the analysis of other author's data favours $\alpha \approx 25 \text{ MeV}^{1/2}$ since one maximum expected at 10 MeV for $\alpha = 29 \text{ MeV}^{1/2}$ is lacking /see Fig. 1/.

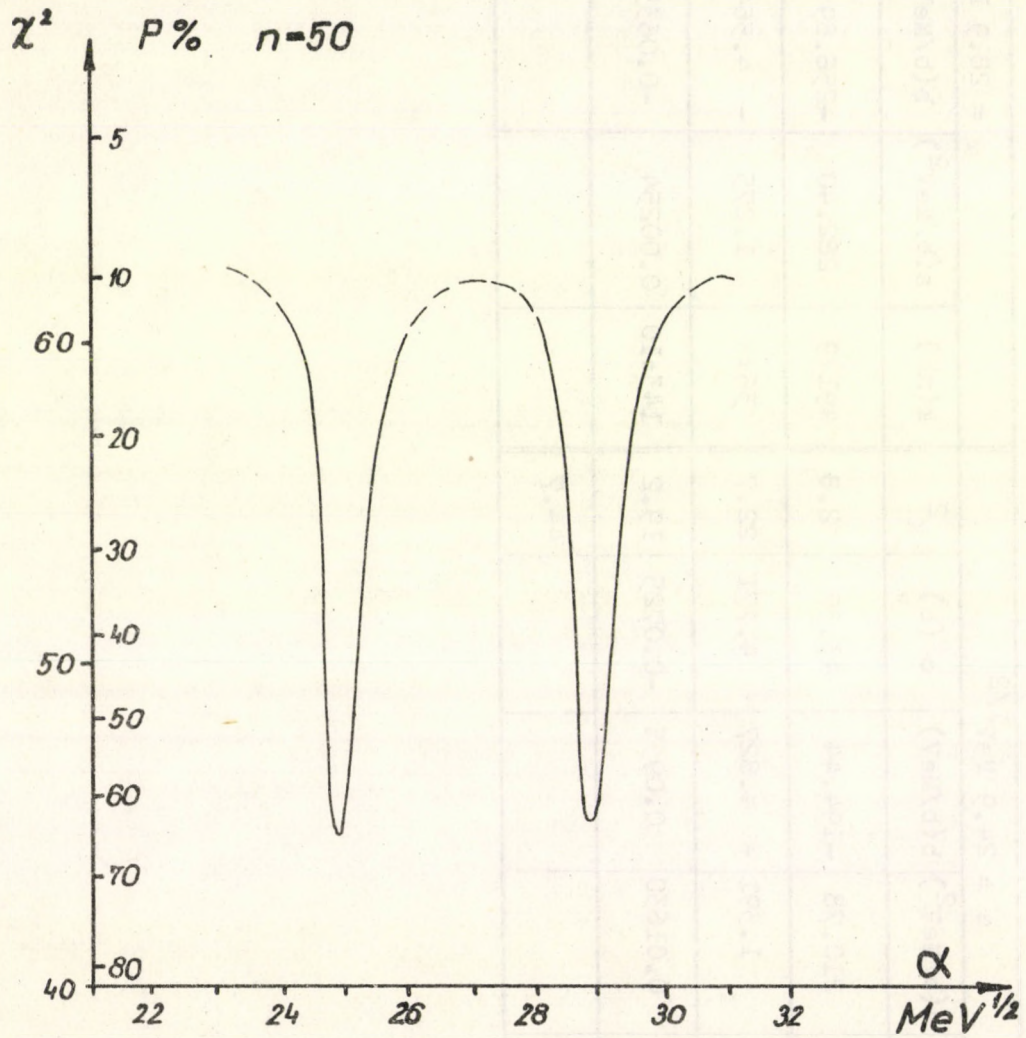


Fig. 6.
The function $\chi^2(\alpha)$ /Eq./47// for the data summarized
in Table 2. and $\sigma_{\text{calc}}(E, \alpha)$ as given by Eq./46/

Table 3.

Energy-region (MeV)	$\alpha = 24.9 \text{ MeV}^{1/2}$					$\alpha = 28.9 \text{ MeV}^{1/2}$				
	k(mb)	a(b/MeV ²)	b(b/MeV)	c (b)	χ^2	k(mb)	a(b/MeV ²)	b(b/MeV)	c(b)	χ^2
0.39-0.47	511±11	210.78	-194.44	43.37	2.8	491±9	282.40	-256.89	60.99	2.7
0.83-1.61	48±9	1.391	- 4.827	4.771	22.7	36±8	1.275	- 4.564	4.635	24.1
2.58-5.24	146±11	0.01630	0.0955	-0.0725	19.2	143±10	0.00254	-0.0633	0.250	18.5
Total					44.7					45.3

4.2. Our next step was to investigate the very interesting question whether the fluctuating cross-section contribution is confined to some restricted angular interval or it is extended uniformly over the whole 4π solid angle. Instead of performing a rather tedious direct angular-distribution measurement the energy spectra dn/dE_p of the recoil protons have been measured at different neutron energies E_n ranging from 2.7 MeV to 5.3 MeV as in one of our previous measurements.

The differential cross-section in center-of-mass system is given by $\sigma(\theta_p) = E_p (dn/dE_p)_{E_p}(\theta_p) / (4\pi\phi N)$ where θ_p is the c.m. angle of proton emission, $E_p(\theta_p) = E_n \cos^2 \theta_p / 2$ is the corresponding proton energy /in lab.system/, ϕ is the integral neutron flux /in neutron per cm^2 / at a thin scatterer which contains N hydrogen atoms. Any energy-dependent departure from the isotropy in the angular distribution can be traced as a corresponding distortion of the proton energy-distribution dn/dE_p . In practical cases, however, the true shape and the intensity of the energy spectra is uncertain to some extent because of distortion factors to be discussed later and of difficulties, respectively, which arise in connection with a reliable determination of the neutron flux. Fortunately, all distortion factors depend smoothly and slowly on the neutron energy, therefore quickly varying distortions, if can be developed by a suitable comparison of the spectra measured.

The proton energy distributions have been measured by means of a scintillation counter consisting of a small trans-stylben crystal viewed by a DuMont 6292 photomultiplier. The crystal was of cylindrical shape /0.8 cm in diameter and 1.0 cm long/ and it was mounted in a thin copper housing, surrounded by MgO as reflector. In the energy region investigated any distortion due to n, α , charged particle/ reactions of the surrounding elements and to the carbon content of the crystal was found negligible. Care was taken of minimizing the proportion of neutrons in-scattered from the surroundings. The neutron-source target arrangement was the same as previously and the neutron energy was varied again by changing the angle θ_n /see Fig 4./, at a fixed bombarding deuteron energy. The source-crystal distance was 25 cm.

In such an experiment it is very important to eliminate the γ - background which may distort the measured spectra seriously and, in addition, the γ -intensity may fluctuate quite rapidly with the neutron energy. We made use of the pulse-shape-discrimination technics in its space-charge controlled version [31]. The separation threshold for protons and fast electrons was found as somewhat below 0.5 MeV electron energy /equivalent to about 1,8 MeV proton energy/, in good agreement with Owen's result [31].

After amplification, both the separation- and the energy-pulses were analyzed simultaneously by a 4096 channel analyser /NTA-4096 typ./ working in two-dimensional /32x128/ setting. Fig 7. shows an illustrative example for how this system operates, at $E = 5$ MeV neutron energy. The S- and U-axes correspond to the separation and the energy-pulse amplitudes, respectively. The discrimination line lies along the middle of the valley between the mountains. In such a way the best possible proton-gamma discrimination could be established.

The amplitude-resolution in the energy-channel was 15 % for neutrons of 5.2 MeV energy and followed the rule (U in channels)

$$\Delta U/U \approx 1.5 U^{-1/2} + 0.01$$

Proton amplitude-distributions have been measured in three runs each ranging over the same ten neutron energies from 2.72 MeV to 5.24 MeV. The total number of counts detected above the $p-\gamma$ discrimination threshold was in the order of 10^5 in each of the spectra and this could be accomplished in about 30 minutes. The overall stability of the measuring system proved to be satisfactory and the spectra measured at the same neutron energy but in different runs were fairly consistent.

The response-energy function of our crystal could be determined with a considerable accuracy by means of the spectra themselves in the following way. Assuming a Gaussian-distribution to express the finite resolution of the detector, and an isotropical angular-distribution for

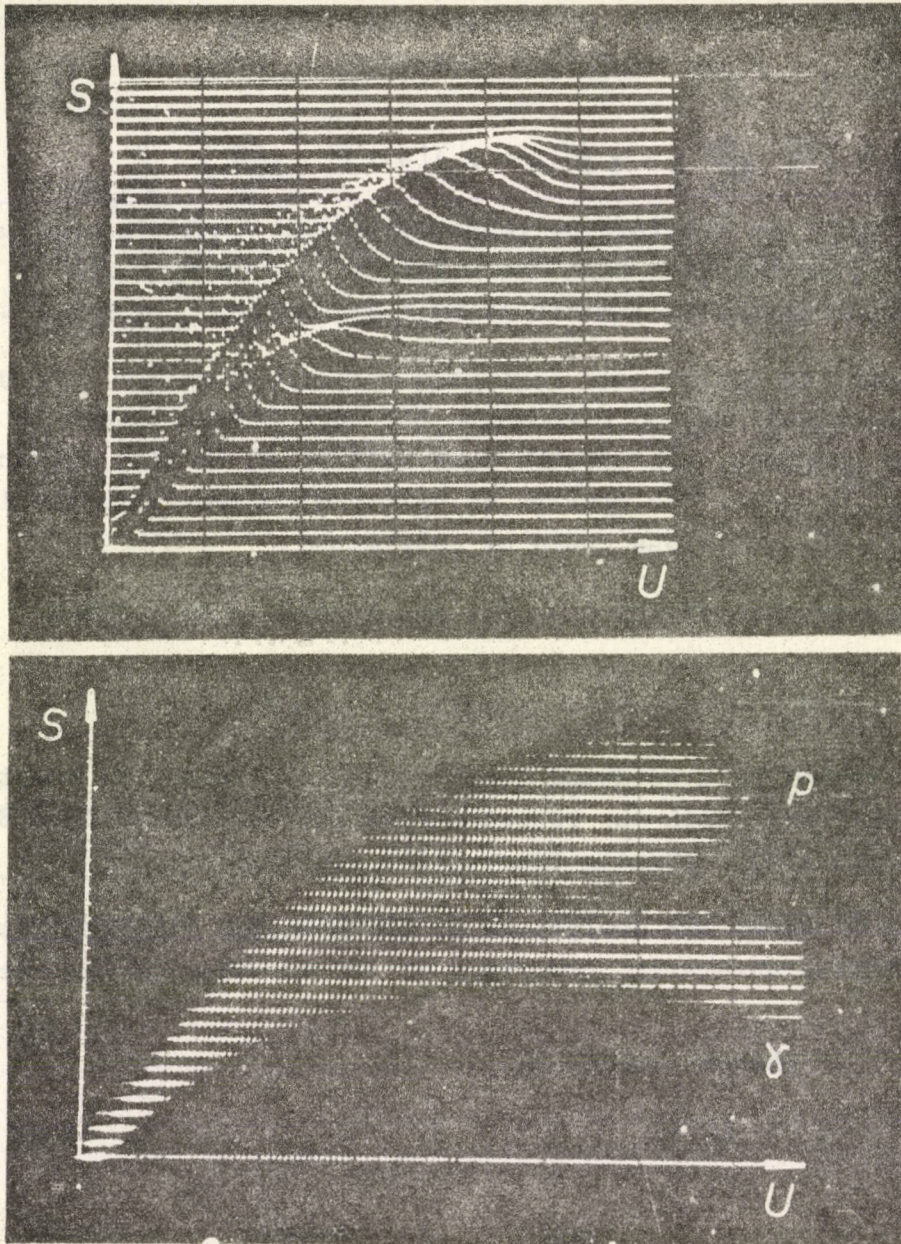


Fig. 7

Two-dimensional /axometric and intensity-modulated/ representations of the channel content of the analyser when measuring recoil-proton energy distribution at 5 MeV neutron energy. For details see text

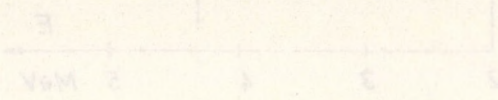


Fig. 8

The deviations of the measured response data from a best fitting quadratic expression as given by Eq. (2) at different proton/neutron energies. Note the occurrence of maximum deviations where fluctuation maxima are expected

the recoil protons in c.m. system /i.e. $dn/dE_p = \text{constant}$ for $0 < E_p < E$ / the amplitude distribution takes the form

$$\frac{dn}{dU} = \left[\frac{1}{2} \frac{dn}{dE_p} \left\{ 1 + \int [(E - E_p)] a\sqrt{2} \right\} \left(\frac{dU}{dE_p} \right)^{-1} \right]_{E_p(U)} \quad /48/$$

where $E_p(U)$ is the inverse response-energy function, $\int(x) \equiv 2^{-1/2} \text{erf } x$ is the error-integral with the argument $x = (E - E_p) \cdot a\sqrt{2}$ and $a^{-1} 2\sqrt{\ln 2}$ is the full-width at half-maximum at $E_p \approx E$.

First, an approximate derivated response-function $(dU/dE_p)_0$ was determined and, to compensate the edge-shifts caused by the non-linear response, all spectra were multiplied by this common function $[(dU/dE_p)_0]_{E_p(U)}$. The spectra so corrected approximate the ideal shape and the edge-positions could be determined.

The response-energy data fit the quadratic expression

$$U(E_p) = 2.52 (E_p^2 + 2.365 E_p + 0.008) \quad /49/$$

as determined by a weighted least square analysis. The function agrees reasonably well with the response-function calculated from Birks's expression [30], assuming there $kB = 0.0120$.

Fig 8. shows the deviations of our measured response data from the best fitting quadratic form /51/, in the function of the energy.

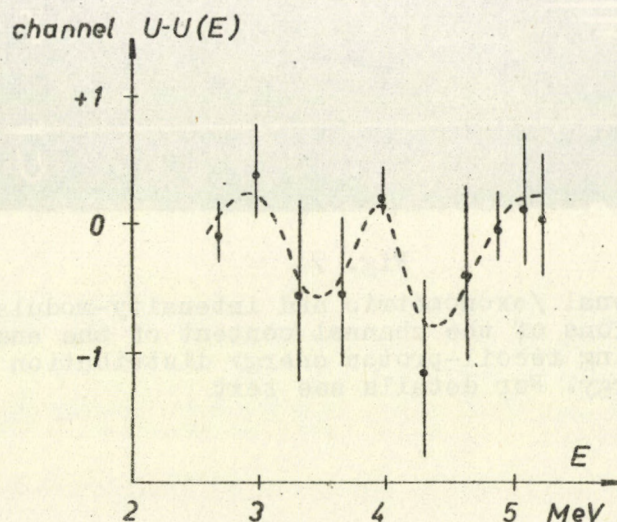


Fig 8.

The deviations of the measured response data from a best fitting quadratic expression as given by Eq/51/ at different proton /neutron/ energies. Note the occurrence of maximum deviations where fluctuation-maxima are expected

The c.m. differential cross-section was calculated using the expression

$$\sigma\left(\theta = \frac{\theta_1 + \theta_2}{2}\right) \approx \text{constant} \cdot \frac{s(\theta_1, \theta_2)}{\left(\cos \frac{\theta_1}{2} - \cos \frac{\theta_2}{2}\right) \cos \frac{\theta_1 + \theta_2}{4}} \quad /50/$$

where $s(\theta_1, \theta_2)$ is the sum of the counts between the limits $U_1 = U(E_p = E \cos^2 \theta_1 / 2)$ and $U_2 = U(E_p = E \cos^2 \theta_2 / 2)$ of all uncorrected spectra measured at the same neutron energy.

Because of the $p - \gamma$ discrimination threshold only a limited angular region as seen in Table 4. could be evaluated. In Table 4. the relative cross-section $\sigma(\theta) / \sigma(50^\circ)$ is given for different neutron energies since this ratio is independent of the /undetermined/ neutron flux. If the limits U_1 and U_2 often happened to fall far from an integer number, in such cases the corresponding fraction of the channel content was taken into account. The errors of the cross-section data refer to the assumption that each sum $s(\theta_1, \theta_2)$ can be determined with an uncertainty corresponding to $\pm 1/2$ of one channel content. Compared with this, the statistical errors are negligible.

Fig 9. shows the energy-dependence of the differential cross section at fixed angles θ . As for the angles $\theta > 30^\circ$, no significant energy-dependence can be found and the angular distribution is isotropic, as it was known.

An entirely different behaviour can be observed, however, in the forward angular region $0 < \theta < 20^\circ$. At these low angles the differential cross-section fluctuates with the energy just in the same way as $\sigma_{np}(E)$ does. Apart from some slight shift the maxima and minima shown in Figs 5c., 9., and also in Fig 1. correspond to each other quite closely, though they were measured in a completely different way. Even in Fig. 8 where the response-energy data are compared to a smooth quadratic function, shows the same structure indicating that at forward angles and in fluctuation maxima there should be an excess of protons with respect to their average intensity.

θ_1 /degrees/	0	20	60	80
θ_2	20	40	80	90
θ /degrees/	10	30	70	85
E (MeV)	$\sigma(\theta)/\sigma(50^\circ) \pm \Delta[\sigma(\theta)/\sigma(50^\circ)]$			
2.72 ± 0.11	1.855 ± 0.195	0.909 ± 0.116	-	-
3.01 ± 0.11	2.037 ± 0.187	0.835 ± 0.093	-	-
3.33 ± 0.11	1.613 ± 0.152	0.896 ± 0.079	1.008 ± 0.056	-
3.69 ± 0.11	1.690 ± 0.115	0.907 ± 0.064	0.976 ± 0.041	0.965 ± 0.084
4.01 ± 0.10	1.720 ± 0.136	0.946 ± 0.063	0.992 ± 0.045	0.976 ± 0.092
4.34 ± 0.09	1.347 ± 0.102	0.903 ± 0.054	0.973 ± 0.037	0.984 ± 0.081
4.65 ± 0.08	1.376 ± 0.100	0.908 ± 0.046	0.974 ± 0.032	0.970 ± 0.068
4.91 ± 0.06	1.395 ± 0.076	0.949 ± 0.038	0.956 ± 0.025	0.938 ± 0.053
5.10 ± 0.04	1.269 ± 0.082	0.977 ± 0.040	0.919 ± 0.025	0.883 ± 0.052
5.24 ± 0.01	1.320 ± 0.080	0.971 ± 0.037	0.924 ± 0.023	0.852 ± 0.046

Table 4.

The measured relative differential cross-sections $\sigma(\theta)/\sigma(50^\circ)$ for neutron-proton scattering at different c.m. angles θ of proton emission and laboratory-energies E . The energy errors are calculated from reaction kinematics, for the cross-section errors see text

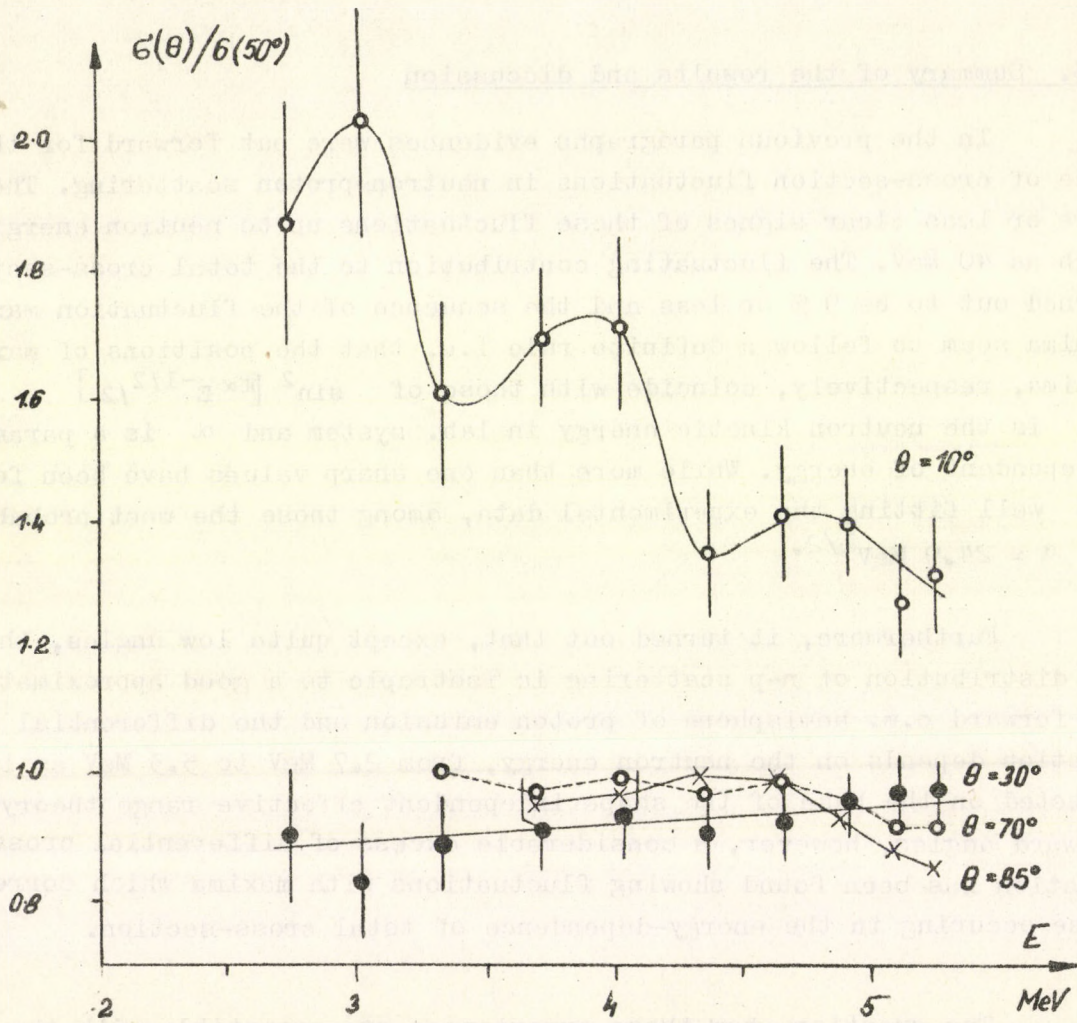


Fig 9
The measured differential cross-section data
 $\sigma(\theta, E) / \sigma(50^\circ, E)$ plotted as a function of the
neutron energy E .

Unfortunately, this measurement could not be extended to backward angles /in c.m. frame of reference/, because of technical difficulties, and we do not know whether similar phenomena exist in that region too.

5 §. Summary of the results and discussion

In the previous paragraphs evidences were put forward for the existence of cross-section fluctuations in neutron-proton scattering. There are more or less clear signs of these fluctuations up to neutron energies as high as 40 MeV. The fluctuating contribution to the total cross-section turned out to be 9 % or less and the sequence of the fluctuation maxima and minima seem to follow a definite rule i.e. that the positions of maxima and minima, respectively, coincide with those of $\sin^2 [\pi \alpha E^{-1/2}/2]$ where E is the neutron kinetic energy in lab. system and α is a parameter independent of energy. While more than one sharp values have been found for α well fitting the experimental data, among those the most probable one is $\alpha = 24.9 \text{ MeV}^{1/2}$.

Furthermore, it turned out that, except quite low angles, the angular distribution of n-p scattering is isotropic to a good approximation in the forward c.m. hemisphere of proton emission and the differential cross-section depends on the neutron energy, from 2.7 MeV to 5.3 MeV as it was expected on the base of the shape independent effective range theory. At forward angles, however, a considerable excess of differential cross-section has been found showing fluctuations with maxima which correspond to those occurring in the energy-dependence of total cross-section.

The question, how these experiences are compatible with the measurements of other authors can be answered partly by quoting the results of § 2. These are summarized in Table 1. and in Fig 1. On the other hand, the recent parameter value r_s to the effective range formula Eq/43/, as given by H.P. Noyes [3], were determined by using 8 selected data on the total cross-section below 5 MeV which, except one at 3.205 MeV, fell by chance into the regions where the fluctuations happened to rise over their half-maxima. Therefore a nearly homogenous set of data had been used. Probably the presence of the fluctuations would explain why the error of r_s could not be improved significantly in Noyes's calculations when using 20 more data on σ_{np} .

As for the differential cross-section measurements in the MeV region, the situation is somewhat embarrassing for the first sight, since it is generally assumed that the angular distribution is isotropic in this energy region. However, no critical review or compilation of data, like that of Hess [14] for higher energies, could be found. In an attempt [32] to have some better insight it has been pointed out that the experimental evidences for isotropy below 9 MeV are not unambiguous enough so as to be incompatible with what has been found here.

Our experiences can be explained in terms of a quite simple model of charge-exchange processes outlined in the first two paragraphs of this paper. Quantitatively, when using a dipole approximation for the interaction matrix-element to the analogy of that of electromagnetic transitions, one finds a realistic, though a bit small value as 0.068 for the dimensionless pion-nucleon coupling constant $f^2/\kappa c$ if $\alpha = 24.9 \text{ MeV}^{1/2}$ is assumed, and 0.090 for the somewhat less significant value $\alpha = 28.9 \text{ MeV}^{1/2}$ /see Eq/33//.

A less definite statement can be given about the amplitude K of the fluctuations. In the MeV region, they are probably higher than suggested originally in § 2. /see Eq/34//, a quantitative rule, however, has not been found as yet.

The authors wish to express their thanks to Mrs. A.Simon for taking responsibility for most of the numerical calculations, and also for her helpful assistance during the experimental work. The authors are also indebted to Dr. I.Borbély, Dr. L.Pócs and Dr. M.Zimányi for their invaluable helps and to Dr. L.Keszthelyi for his encouraging support from the very beginning of this work.

References

- [1] A.A.Vuylsteke: Elements of Maser Theory, VanNostrand Co., 1960.p.177.
- [2] S.DeBenedetti: Nuclear Interactions, John Wiley and Sons, Inc. New York, London, Sydney /1964/ Sect.3.15,p.159.
- [3] H.P.Noyes: Phys.Rev. 130 /1963/, 2025
- [4] Атлас эффективных нейтронных сечений элементов, Ак. Наук СССР, 1955.
- [5] R.E.Fields et al.: Phys.Rev. 94 /1954/, 389.
- [6] C.L.Storrs and D.H.Frisch: Phys.Rev. 95 /1954/, 1252.
- [7] E.E.Lampi et al.: Phys.Rev. 76 /1949/, 188.
- [8] R.E.Fields et al.: Phys.Rev. 89 /1953/, 908.
- [9] W.Sleator: Phys.Rev. 72 /1947/, 207.
- [10] N.Nereson and S.Darden: Phys.Rev. 89 /1953/, 775.
- [11] C.E.Engelke et al.: Phys.Rev. 129 /1963/, 324.
- [12] M.Ageno et al.: Phys.Rev. 71 /1947/, 20.
- [13] E.M.Hafner et al.: Phys.Rev. 89 /1953/, 204.
- [14] W.N.Hess: Rev.Mod.Phys. 30 /1958/, 368.
- [15] L.S.Goodman: Phys.Rev. 88 /1952/, 686.
- [16] E.O.Salant and N.F.Ramsay: Phys.Rev. 57 /1940/, 1075.
- [17] H.L.Poss et al.: Phys. Rev. 87 /1952/, 11.
- [18] C.F.Cook and T.W.Bonner: Phys.Rev. 94 /1954/, 651.
- [19] H.L.Poss et al.: Phys.Rev. 85 /1952/, 703.
- [20] J.H.Coon et al.: Phys.Rev. 88 /1952/, 562.
- [21] P.H.Bowen et al.: Nucl.Phys. 22 /1961/, 640.
- [22] R.B.Day and R.H.Henkel: Phys.Rev. 92 /1953/, 358.
- [23] R.B.Day et al.: Phys.Rev. 98 /1955/, 279.
- [24] R.Sherr: Phys.Rev. 68 /1945/, 240.
- [25] A.E.Taylor and E.Wood: Phyl.Mag. 44 /1953/, 95.
- [26] R.H.Hildebrand and C.E.Leith: Phys.Rev. 80 /1950/. 842.
- [27] V.Culler and R.W.Waniek: Phys.Rev. 95 /1954/, 585.
- [28] G.R.Mott et al.: Phys.Rev. 88 /1952/, 9.
- [29] R.A.J.Riddle et al.: Nucl.Phys. 61 /1965/, 457.

- [30] J.B.Birks: The Theory and Practice of Scintillation Counting, Pergamon Press, 1964.
- [31] R.B.Owen: Nucleonics 17 No9 /1959/, 92.
- [32] T.Czibók: KFKI Közlemények 16, /1968/, 401
- [33] M.D.Goldberg et al.: Angular Distributions in Neutron Induced Reactions Vol.I. BNL 400, 2nd Edition October 1962, 1-0-1 ff.

[30] J.F. Birk: The Theory and Practice of Scintillation Counting, Pergamon Press, 1964.

[31] R.B. Owen: Nuclear Science 17 No. 1958, 95.

[32] T. Ostörk: KFKI Közlemények 48, 1958, 403.

[33] M.D. Goldberg et al.: Angular Distributions in Neutron Induced Reactions Vol. I, IAEA, 2nd Edition October 1962, 1-0-1 11.

Printed in the Central Research Institute for Physics, Budapest

Kiadja a Könyvtár- és Kiadói Osztály. O.v.: dr. Farkas Istvánné
Szakmai lektor: dr. Keszthelyi Lajos. Nyelvi lektor: Kovács Jenőné
Példányszám: 170 Munkaszám: 4349 Budapest, 1969. március 27.
Készült a KFKI házis sokszorosítójában. F.v.: Gyenes Imre

~~61~~

61 811

Printed in the Central Research Institute for Physics, Budapest
Kiadja a Könyvtár- és Kiadó Osztály, O. v. t. dr. Farkas Istvánné
Gazdálkodó: dr. Kezdegyi János, Nyelvi felelős: Kovács Teréz
Felelős: IV. Budapest, 1989. március 27.
Kiadja a KFKI Részecskefizikai Intézet, P. v. t. Győző Imre

